CANCER

Transient CDK4/6 inhibition protects hematopoietic stem cells from chemotherapy-induced exhaustion

Shenghui He,[1,2]* Patrick J. Roberts,[3]* Jessica A. Sorrentino,[3] John E. Bisi,[3] Hannah Storrie-White,[3] Renger G. Tiessen,[4] Karenann M. Makhuli,[3] William A. Wargin,[5] Henko Tadema,[4] Ewoud-Jan van Hoogdalem,[4] Jay C. Strum,[3] Rajesh Malik,[3] Norman E. Sharpless[1,2]†

Conventional cytotoxic chemotherapy is highly effective in certain cancers but causes dose-limiting damage to normal proliferating cells, especially hematopoietic stem and progenitor cells (HSPCs). Serial exposure to cytotoxics causes a long-term hematopoietic compromise ("exhaustion"), which limits the use of chemotherapy and success of cancer therapy. We show that the coadministration of G1T28 (trilaciclib), which is a small-molecule inhibitor of cyclin-dependent kinases 4 and 6 (CDK4/6), contemporaneously with cytotoxic chemotherapy protects murine hematopoietic stem cells (HSCs) from chemotherapy-induced exhaustion in a serial 5-fluorouracil treatment model. Consistent with a cell-intrinsic effect, we show directly preserved HSC function resulting in a more rapid recovery of peripheral blood counts, enhanced serial transplantation capacity, and reduced myeloid skewing. When administered to healthy human volunteers, G1T28 demonstrated excellent in vivo pharmacology and transiently inhibited bone marrow (BM) HSPC proliferation. These findings suggest that the combination of CDK4/6 inhibitors with cytotoxic chemotherapy should provide a means to attenuate therapy-induced BM exhaustion in patients with cancer.

INTRODUCTION

Human bone marrow (BM) is sensitive to cell cycle–dependent cytotoxic agents, and myelosuppression is the dose-limiting toxicity for most such agents. Myelosuppression causes life-threatening morbidity, augments the cost of care, and compromises therapeutic efficacy, through the induction of treatment delays and reduced therapeutic intensity. It has further been suggested that cytotoxic chemotherapy induces lasting immunosuppression that dampens a beneficial antitumor immune response (*1*). The long-term BM toxicity of cytotoxics is also a major problem for cancer survivors because it is associated with serious late toxicities of cancer therapy: BM exhaustion, myelodysplastic syndrome (MDS), and acute leukemia. Whereas the depletion of committed hematopoietic progenitor cells (HPCs) is largely responsible for the acute hematopoietic toxicity of chemotherapy, damage and functional attrition of hematopoietic stem cells (HSCs) contribute to therapy-induced late myelotoxicity (*2*–*5*).

Existing strategies to manage chemotherapy-induced myelosuppression focus on correcting acute cytopenias through the transfusion of platelets and red blood cells and the administration of growth factors: granulocyte colony-stimulating factor (G-CSF) or erythropoietin (EPO). Transfusions decrease quality of life during therapy and are associated with transfusion reactions and risk of infection. Although growth factors ameliorate acute myelosuppression, their use is problematic in that they have substantial acute toxicity of their own (for example, excess mortality and thrombosis for EPO and fever and bone pain for G-CSF), adverse long-term consequences manifesting as exacerbated HSC exhaustion (*6*, *7*), and an increased risk for MDS and leukemia (*8*, *9*). To date, no therapeutic option is available to prevent or treat chemotherapy-induced functional exhaustion of HSCs.

It has long been suggested that selective inhibition of the proliferation of normal but not cancer cells may provide protection from chemotherapy-induced toxicity (*10*, *11*), but an incomplete understanding of cell cycle regulation has prevented the reduction of this concept to practice. We and others have shown that hematopoietic stem and progenitor cells (HSPCs) depend on cyclin-dependent kinases 4 and 6 (CDK4/6) activity for proliferation (*12*–*14*), whereas many human cancers are resistant to CDK4/6 inhibition [for example, retinoblastoma (RB)–deficient cancers] (*15*, *16*). This suggests that coadministration of a CDK4/6 inhibitor (CDK4/6i) with cytotoxic chemotherapeutic agents could augment the therapeutic window by protecting normal HSPCs without negating the antineoplastic effect against CDK4/6-independent tumors. Using a long-acting oral CDK4/6i, we previously showed that a transient period of "pharmacological quiescence" (PQ) can reduce platinum chemotherapy–induced acute myelosuppression in vivo (*17*). It is unclear, however, whether long-term BM toxicities of chemotherapy can be attenuated by PQ.

G1T28 (trilaciclib) is a small-molecule CDK4/6i developed for reducing chemotherapy-induced myelosuppression (*18*). This molecule affords excellent in vivo protection against DNA-damaging agents in rodent models and has favorable potency, selectivity, and pharmacological properties for this purpose (*18*). In particular, G1T28 is well suited for chemoprotection applications, which require an agent with a short biological half-life and intravenous formulation. Here, we examine the ability of G1T28 to modulate HSPC proliferation and preserve long-term HSC function in humans and mice.

RESULTS

G1T28 induces transient and reversible G_1 cell cycle arrest in murine HSPCs

We first determined the pharmacodynamic (PD) response of murine HSPCs to G1T28 using 5-ethynyl-2′-deoxyuridine (EdU) incorporation assay (figs. S1 to S4), focusing on dose and schedule. A single intraperitoneal

[1]Departments of Genetics and Medicine, University of North Carolina School of Medicine, Chapel Hill, NC 27599–7295, USA. [2]Lineberger Comprehensive Cancer Center, University of North Carolina School of Medicine, Chapel Hill, NC 27599–7295, USA. [3]G1 Therapeutics Inc., Research Triangle Park, NC 27709, USA. [4]PRA Health Sciences, P.O. Box 200, 9470 AE Zuidlaren, Netherlands. [5]Nuventra Pharma Sciences, Research Triangle Park, NC 27713, USA.
*These authors contributed equally to this work.
†Corresponding author. Email: nes@med.unc.edu

dose of G1T28 was sufficient to induce a dose-dependent reduction in EdU incorporation (S-phase cells) in all hematopoietic cell types at 12 hours after treatment (Fig. 1, A to C, and figs. S2 and S3) without causing other cell cycle effects such as G_2-M arrest (fig. S2) or acute cytotoxicity (fig. S4C). This G1T28-induced reduction in S-phase cell frequency was independently confirmed using DNA content analysis (figs. S3B and S4B). HSCs, early HPCs [$Lin^-Sca\text{-}1^+c\text{-}Kit^+$ (LSK) cells and myeloid progenitors (MPs)], and developing lymphoid cells were the most sensitive to CDK4/6i-induced G_1 arrest, showing a significantly lower median effective dose (ED_{50}) (Fig. 1B; $P < 0.001$) for G1T28 and a more complete G_1 cell cycle arrest (Fig. 1C; $P < 0.05$) compared to maturing erythroid and myeloid cells.

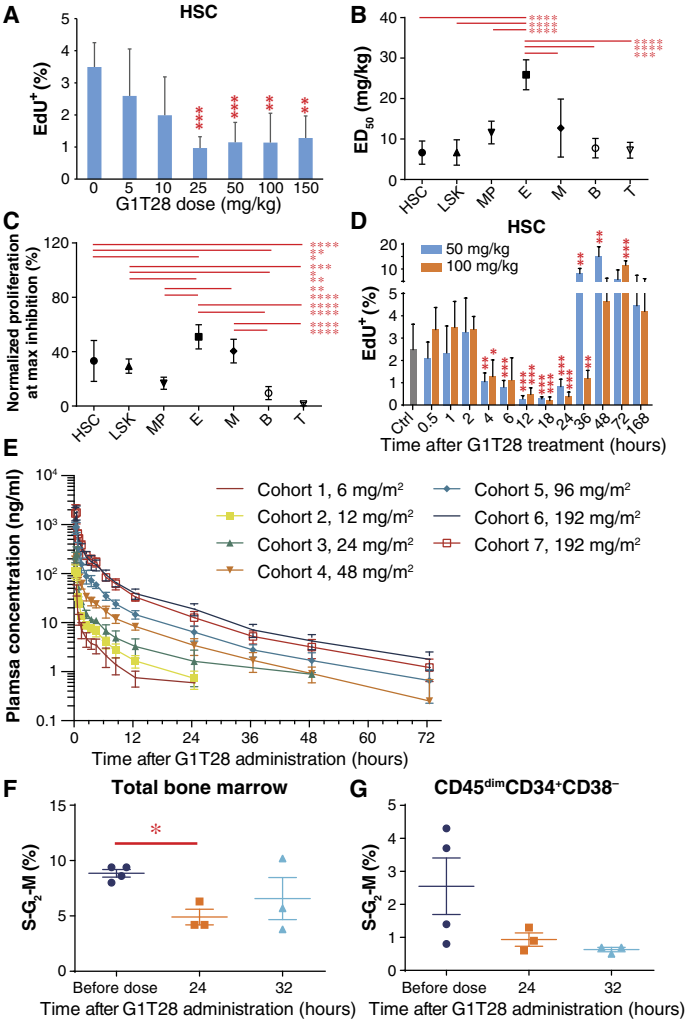

Fig. 1. G1T28 induces transient, reversible G_1 cell cycle arrest in both murine and human BM HSPCs. (**A**) Rate of murine BM HSC proliferation 12 hours after a single intraperitoneal injection of the indicated doses of G1T28 [n = 5 mice per dose analyzed in five independent experiments, same for (B) and (C)]. (**B**) ED_{50} of G1T28 to inhibit the in vivo proliferation of the indicated murine hematopoietic cell types with identification scheme shown in fig. S1. E, erythroid; M, myeloid; B, B lymphocytes; T, T lymphocytes. (**C**) Relative proliferation rate of each murine hematopoietic cell type at maximum (max) CDK4/6 inhibition, compared to untreated mice. (**D**) Rate of murine BM HSC proliferation at various time points after a single intraperitoneal injection of 50 or 100 mg/kg of G1T28 (n = 3 to 6 mice per dose per time point). Ctrl, control. (**E**) Mean plasma concentration curve of G1T28 after single-dose intravenous administration in healthy human volunteers. (**F** and **G**) Frequency of total human BM cells (F) and HSC-enriched $CD45^{dim}CD34^+CD38^-$ BM cells (G) in S-G_2-M phase of the cell cycle either before or at 24 and 32 hours after single dose of G1T28 treatment. Data were from cohort 7 (BED) after a single dose (192 mg/m^2) of G1T28. Error bars represent SD in (A) to (D) and SEM in (E) to (G). The statistical significance of differences between vehicle- and G1T28-treated groups in (A) and (D) and between indicated groups in (B), (C), and (F) was assessed using unpaired two-tailed Student's t tests (*P < 0.05, **P < 0.01, ***P < 0.001, ****P < 0.0001).

The cell cycle arrest induced by G1T28 was transient, reversible, and dose-related (Fig. 1, A to D, and figs. S3 and S4, B and D to J). In HSCs, a reduction in EdU incorporation and S-G_2-M cell frequency was seen as early as 4 hours after G1T28 treatment, reaching the minimum at 12 hours and lasting up to 36 hours before recovery (Fig. 1D and fig. S4B). Doses of G1T28 above 50 mg/kg did not cause a further reduction in EdU incorporation (Fig. 1A and fig. S3, C to I) but rather extended the duration of cell cycle arrest (Fig. 1D and fig. S4, B and D to J), consistent with the measured pharmacokinetics (PK) of G1T28 in mice (fig. S5). Notably, CDK4/6 inhibition not only reduced homeostatic proliferation of HSCs (Fig. 1, A and D, and figs. S3B and S4B) but also abrogated the potent cell cycle entry of HSCs seen during recovery from cytotoxic myeloablation (fig. S3J), which is essential for maintaining HSC cycle arrest during prolonged chemotherapy treatment.

The duration of the G1T28-induced cell cycle arrest differed by hematopoietic cell types, correlating inversely with the sensitivity of each cell type to CDK4/6 inhibition: T cells > HSPCs ≥ B cells > maturing myeloid and erythroid cells (Fig. 1D and fig. S4, D to J). Notably, the proliferation rates of most hematopoietic cell types increased beyond steady state during the early period of recovery (Fig. 1D and fig. S4, B and E to J), likely reflecting compensatory proliferation in response to the transient mild reduction of BM cellularity as a result of HSPC cycle arrest (fig. S4C).

G1T28 also induces a transient, reversible G_1 arrest of human HSPCs

To determine whether G1T28 can induce a similar transient and reversible G_1 cell cycle arrest in human HSPCs, as well as to characterize the pharmacological properties and safety of the compound, we completed a first-in-human phase 1 clinical trial in healthy volunteers. In total, 45 subjects were enrolled: 36 received G1T28 in seven dosing groups and 9 received placebo. On average, demographic characteristics (table S1) were comparable among the seven G1T28 groups and the placebo group with regard to mean age, body mass index (BMI), and body surface area (BSA). G1T28 and placebo (5% dextrose solution) were administered as a 30-min intravenous infusion. Of the 33 subjects enrolled in the single ascending dose (SAD) part of the study, 24 received G1T28 at doses of 6, 12, 24, 48, 96, or 192 mg/m^2 and 9 received placebo (table S2). Overall, a single intravenous infusion of G1T28 at all test doses was well tolerated. The most frequently reported treatment emergent adverse events (TEAEs) were headache and nausea (table S3). No TEAEs of severe or life-threatening intensity were reported, and all moderate TEAEs spontaneously resolved within 24 hours. There were no clinically relevant changes in any of the treatment groups with respect to clinical laboratory testing [clinical chemistry, hematology (blood cell counts, including absolute reticulocyte and banded neutrophil counts), and urinalysis], vital signs, electrocardiogram (ECG), physical examination, or body weight.

The PK properties of G1T28 were assessed using standard approaches. After a single intravenous infusion of G1T28 at doses shown in table S2, the median time (t_{max}) to reach peak serum concentration (C_{max}) ranged between 0.25 and 0.47 hours after the start of infusion

(Fig. 1E and table S4). The geometric mean of C_{max} and the estimated area under the curve ($AUC_{0\text{-}t}$ and $AUC_{0\text{-}inf}$) for G1T28 increased in a dose-proportional manner over the dose ranges tested (table S4). The elimination of G1T28 appeared to occur in three phases after the end of infusion: a fast α-phase until about 4 hours, followed by a β-phase until about 36 hours, and a more gradual terminal γ-phase, suggesting a three-compartment model (Fig. 1E). Because the concentrations of the lowest-dose groups fell below the quantifiable limit before the last elimination phase, the terminal half-life ($t_{1/2}$) of the lowest-dose groups was determined by the first elimination phase ($t_{1/2}$ of 5.32 to 9.28 hours). The terminal $t_{1/2}$ of the 48, 96, and 192 mg/m^2 dose groups was determined by the second elimination phase, with a $t_{1/2}$ of 12.9 to 14.7 hours (table S4). However, because the contribution of the terminal phase to the effective half-life of the drug is about 15 to 20%, the longer $t_{1/2}$ at the higher-dose levels is likely to be less relevant. Compartmental analysis at the biologically effective dose (BED) of 192 mg/m^2 demonstrated geometric means for C_{max} and $AUC_{0\text{-}inf}$ of 1705 ng/ml and 2991 hours·ng/ml, respectively (table S4). The coefficients of variability (%) for these values were all ≤15%, demonstrating low intersubject variability. Total systemic exposure was independent of gender, BSA, age, and body weight. These results demonstrate that G1T28 has acceptable in vivo pharmacology for use in human patients.

To determine the effects of G1T28 on human HSPC proliferation, we analyzed the cell cycle status of BM HSPCs in 12 subjects (cohort 7) either before or after G1T28 treatment (BED, 192 mg/m^2). A single BM aspirate was obtained from each subject (before dose, $n = 5$; 24 hours, $n = 3$; 32 hours, $n = 4$), and cell cycle status of total BM, uncommitted BM HSPCs, and lineage-committed BM cells were assessed by cellular DNA content analysis (table S5 and figs. S6 and S7). Total BM cells showed a 45% reduction in S-G_2-M cell frequency at 24 hours with a partial recovery at 32 hours (Fig. 1F). This extent of G1T28-induced total BM cell cycle arrest is in line with murine data (fig. S4D). The effects of G1T28 on the proliferation of different BM cell lineages were also consistent with the murine findings. The percentage of cells in S-G_2-M phase of the cell cycle decreased at 24 hours after G1T28 for all cell populations except the granulocyte lineage (Fig. 1G, fig. S7, and table S5). As in the mouse, the strongest effects were seen on immature HSPCs, with more modest effects on differentiated cells (fig. S7 and table S5). Given that a single dose of G1T28 did not significantly alter peripheral blood (PB) cell counts for up to 14 days after infusion (fig. S8), these data together suggest that G1T28-induced HSPC cycle arrest is transient, reversible, and well tolerated in humans.

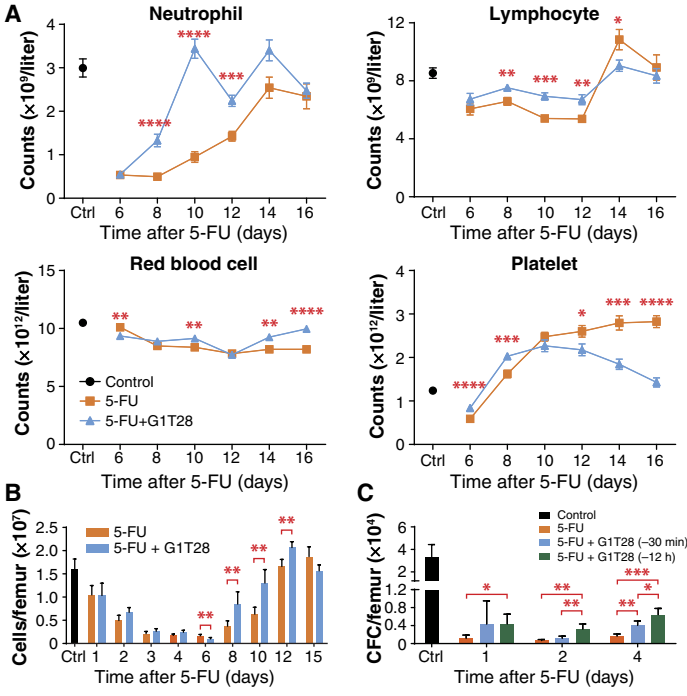

Fig. 2. Transient G_1 arrest by G1T28 pretreatment accelerates hematologic recovery after single-dose 5-FU treatment. (**A** and **B**) Complete blood counts (CBCs) (A) and BM cellularity (B) at various time points after a single dose of 5-FU with or without G1T28 pretreatment (n = 5 to 18 mice per treatment per time point). (**C**) Number of colony-forming cells (CFCs) per femur 1 to 4 days after a single treatment with 5-FU ± G1T28 (n = 4 to 11 mice per treatment per time point). Data represent means ± SEM in (A) and mean ± SD in (B) and (C). The statistical significance of differences between indicated groups was assessed using unpaired two-tailed Student's t tests (*P < 0.05, **P < 0.01, ***P < 0.001, ****P < 0.0001).

Transient G_1 arrest accelerates hematologic recovery after single-dose 5-FU treatment

We next examined the effects of a transient HSPC G_1 arrest on chemotherapy-induced BM exhaustion using 5-fluorouracil (5-FU), a pyrimidine analog toxic to proliferating cells (*19*). Although a single dose of 5-FU causes transient myelosuppression without directly damaging quiescent HSCs (*20*), repeated doses of 5-FU provide a well-characterized model of HSC exhaustion (*21*, *22*). First, to determine the effects of PQ on 5-FU–induced acute myelosuppression, adult C57BL/6 mice were treated with either vehicle or G1T28 30 min before a single injection of 5-FU. 5-FU treatment caused a rapid and transient depletion of all blood cell lineages (Fig. 2A). In accord with published studies (*17*), G1T28 pretreatment did not prevent the initial drop in blood cell counts but significantly accelerated the PB count recovery (Fig. 2A; P < 0.05). Because the acute hematologic toxicity of 5-FU is caused by the depletion of rapidly dividing HPCs (*18*, *20*), we determined the effect of G1T28 treatment on the number of BM progenitors at various time points after 5-FU administration using the methylcellulose colony formation assay. Although G1T28 treatment did not prevent the decline of total BM cell count at 24 hours after 5-FU administration (Fig. 2B), it increased the number of colony-forming cells that survived 1 and 2 days after 5-FU treatment (Fig. 2C), resulting in a faster recovery of the number of colony-forming progenitors (Fig. 2C) and an accelerated recovery of BM cell counts (Fig. 2B). Together, these data indicate that a G1T28-induced transient G_1 cell cycle arrest attenuates the acute hematopoietic toxicity of cytotoxic agents by protecting rapidly proliferating BM progenitors.

Transient G_1 cell cycle arrest protects mice from repeated 5-FU–induced lethal myelosuppression

Single-dose 5-FU treatment causes transient myelosuppression, but repeated administration of 5-FU at relatively short intervals (7 to 10 days) causes irreversible morbidity requiring euthanasia, resulting from incomplete recovery of BM hematopoiesis between treatments (*23*–*25*). To determine whether PQ at the time of each serial dose of 5-FU could afford survival protection, we subjected adult mice to repeated doses of 5-FU at intervals of 7 or 10 days. Twelve hours before (−12 hours) each 5-FU injection, animals received either vehicle or G1T28 (50 or 100 mg/kg). In all cases, G1T28-treated animals exhibited a marked and dose-dependent enhancement in survival compared to vehicle-treated controls (Fig. 3, A and B). At the 100 mg/kg dose, G1T28-treated mice showed a 55% increase in median survival over controls (28 versus 18 days) when

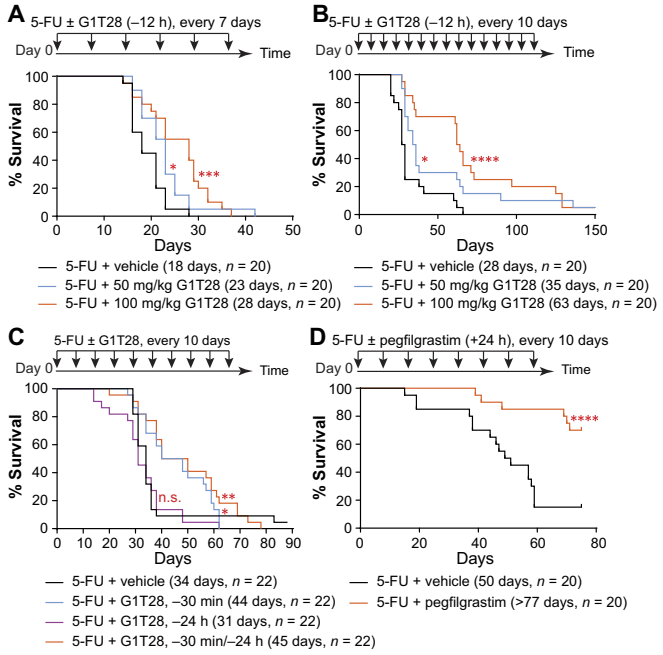

Fig. 3. G1T28 pretreatment protects mice from repeated doses of 5-FU challenge. (**A** to **D**) Survival curves of mice that were treated with 5-FU plus vehicle, G1T28, or pegfilgrastim at 7-day (A) or 10-day (B to D) intervals. G1T28 was given 12 hours before 5-FU in (A) and (B) and either 30 min before, 24 hours before, or both in (C). Pegfilgrastim was given 24 hours after 5-FU in (D). Numbers in parenthesis indicate median survival and animal number (*n*) in each treatment group. Significance for the pairwise comparison to 5-FU + vehicle was calculated using log-rank test in (A), (B), and (D) and Gehan-Breslow-Wilcoxon test in (C) (*$P < 0.05$, **$P < 0.01$, ***$P < 0.001$, ****$P < 0.0001$; n.s., not significant).

5-FU was given at 7-day intervals (Fig. 3A) and a 125% increase in median survival (63 days versus 28 days) when 5-FU was given at 10-day intervals (Fig. 3B). Marked protection was also noted in the 10-day assay when G1T28 was given 30 min before (−30 min) each 5-FU treatment but not when it was given 24 hours before (−24 hours) 5-FU treatment (Fig. 3C). G1T28 given twice, at −24 hours and −30 min, offered no additional protection over treatment at −30 min alone (Fig. 3C). After intraperitoneal injection, 5-FU is rapidly eliminated from the plasma ($t_{1/2}$ = 10 to 20 min) (*26*) and then induces DNA damage for several hours after infusion. Given that the maximum G_1 arrest in HSPCs occurs between 12 and 24 hours after G1T28 treatment (Fig. 1D and fig. S4, B and D to J), the finding of enhanced protection when G1T28 was administered at −30 min or −12 hours, but not −24 hours, suggests that potent protection of HSPCs is best achieved when the period of G_1 arrest overlaps with the in vivo biologic effect of 5-FU treatment. Other structurally distinct CDK4/6is (palbociclib and ribociclib), as well as G-CSF (pegfilgrastim), also demonstrated a survival benefit in this assay (Fig. 3D and table S6). These results suggest that a CDK4/6i-induced G_1 cell cycle arrest provides a substantial reduction in lethal myelosuppression caused by serial administration of a cytotoxic agent.

Transient G_1 arrest by G1T28 at the time of chemotherapy protects murine HSCs from serial 5-FU treatment-induced proliferative exhaustion

Even in the absence of direct cytotoxicity, chemotherapy agents can induce functional attrition of HSCs through a process of proliferative exhaustion. HSCs have an extensive but finite capacity to sustain multilineage hematopoiesis (*27*), and repeated rounds of proliferation (such as during recovery from 5-FU–induced BM ablation) readily exhaust their long-term multilineage reconstitution potential. To determine whether the attenuation of acute chemotherapy–induced myelosuppression by transient G_1 arrest (Fig. 2) can reduce the proliferative burden on quiescent HSCs, thereby extending their functional life span, we assessed the effect of G1T28 on protecting HSCs against serial 5-FU treatment–induced proliferative exhaustion. Young adult B6.SJL ($CD45.1^+$) mice were treated with four rounds of 5-FU ± G1T28 at 3-week intervals (Fig. 4A)—a schedule that causes HSC proliferative exhaustion and premature aging (*22*). As was the case after a single dose of 5-FU (Fig. 2A), CBC analysis after the fourth serial dose of 5-FU showed that the G1T28-treated mice exhibited faster count recovery compared to vehicle-treated controls (fig. S9A). After four rounds of 5-FU followed by count recovery, BM cells were harvested, enumerated, and transplanted, as per Fig. 4A. Consistent with a previous report (*22*), serial 5-FU treatment caused a decrease in BM B cell frequency and an increase in BM HSC frequency, similar to those observed during hematopoietic aging (*28*–*31*), which were not rescued by G1T28 pretreatment (fig. S9, B and C). These observations suggest that, although a transient G_1 arrest at the time of 5-FU administration affords potent protection of PB counts after each cycle, it does not rescue the aging-like phenotypic expansion of HSCs induced by serial 5-FU.

To directly test whether a transient G_1 arrest at the time of each dose of serial 5-FU protects long-term HSC function, we performed competitive BM transplantation assays 8 weeks after the last dose of 5-FU (Fig. 4A). Five hundred thousand BM cells ($CD45.1^+$) harvested from mice treated with 5-FU only or 5-FU + G1T28 were transplanted against an equal number of untreated $CD45.2^+$ BM cells into lethally irradiated C57BL/6 recipients ($CD45.2^+$). The frequencies of donor-derived cells in recipient PB were monitored monthly for 4 months after transplant. Although serial 5-FU treatment significantly reduced the long-term contribution of HSCs to all PB lineages (Fig. 4, B to E; $P < 0.05$), HSCs from G1T28-treated animals demonstrated enhanced reconstitution of all lineages (Fig. 4, B to E; $P < 0.05$). This observation indicates that a transient G_1 arrest induced contemporaneously with serial administration of 5-FU provides a sustained, transplantable attenuation of chemotherapy-induced HSC damage.

Given that growth factor treatment is currently used to address chemotherapy-induced myelosuppression, we also directly compared the effects of G-CSF (pegfilgrastim) treatment with G1T28-induced G_1 arrest on protecting long-term HSC function from serial 5-FU–induced damage. Although pegfilgrastim enhanced survival against serial 5-FU treatment at short intervals, presumably by stimulating the proliferation of surviving MPs (Fig. 3D and table S6), pegfilgrastim treatment 24 and 48 hours after each cycle of 5-FU treatment did not benefit long-term HSC function. In fact, G-CSF treatment further reduced the long-term multilineage reconstitution potential of HSCs compared to 5-FU treatment alone (Fig. 4, B to E). Moreover, the combined use of pegfilgrastim with G1T28 abolished the HSC-protective effect of G1T28 (Fig. 4, B to E). These data are in line with previous reports that G-CSF treatment exacerbates HSC injury after irradiation (*32*, *33*) and findings that its use is associated with an increased later risk of myelodysplasia or leukemia (*8*, *9*).Therefore, although G-CSF can accelerate the acute hematologic recovery after BM injury, it appears to also exacerbate HSC exhaustion (*7*), likely due to disrupting HSC-niche interaction that results in HSC mobilization and proliferation (*34*). In contrast, the PQ approach by CDK4/6i appears to benefit both acute count recovery and long-term HSC function.

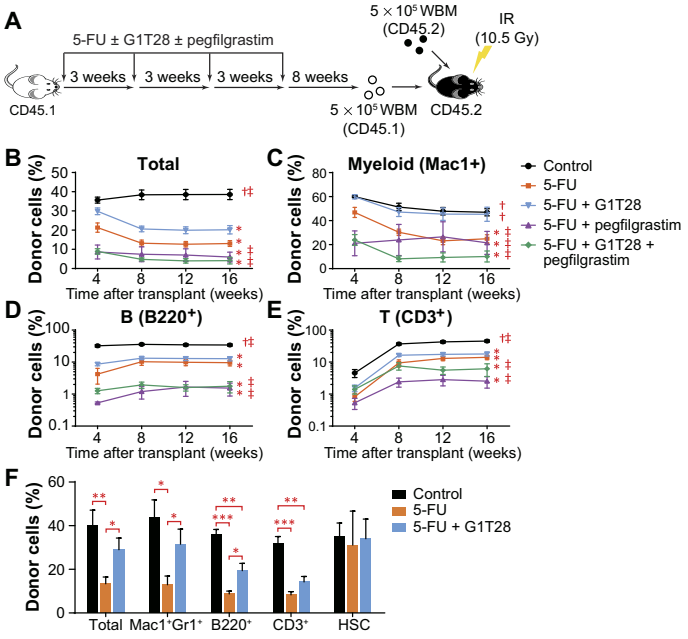

Fig. 4. G1T28-induced PQ protects HSCs from proliferative exhaustion. (**A**) Treatment and BM transplantation schematic. WBM, whole bone marrow cells. IR, ionizing radiation. (**B** to **E**) Percentage of donor-derived cells (CD45.1$^+$) in total PB leukocytes (B) or myeloid cell (Mac1$^+$) (C), B lymphocyte (B220$^+$) (D), and T lymphocyte (CD3$^+$) (E) fractions 1 to 4 months after primary BM transplantation (n = 3 to 8 donor mice per treatment and 5 recipients per donor). Statistical significance of differences between treatment groups at 16 weeks after transplantation was assessed using one-way analysis of variance (ANOVA) with correction for multiple comparisons (*P < 0.05 compared to control, $^{\dagger}P$ < 0.05 compared to 5-FU + vehicle, and $^{\ddagger}P$ < 0.05 compared to 5-FU + G1T28). (**F**) Percentages of donor-derived cells in total BM cells, HSCs, and major BM cell lineages 32 weeks after BM transplantation (n = 5 donor mice per treatment and 5 recipients per donor). Statistical significance was assessed by two-tailed Student's t test (*P < 0.05, **P < 0.01, ***P < 0.001). Average donor cell reconstitution in (B) to (F) was calculated by first averaging the value of the five recipients from each donor, followed by calculating the means of all donors. Error bars represent SEM.

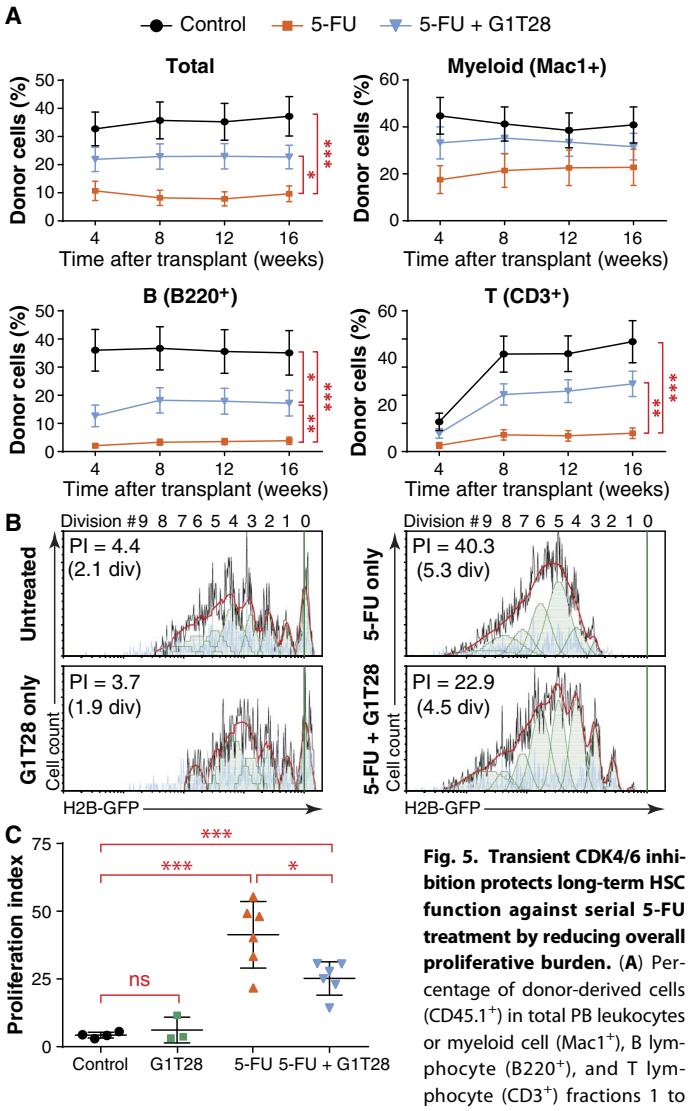

Fig. 5. Transient CDK4/6 inhibition protects long-term HSC function against serial 5-FU treatment by reducing overall proliferative burden. (**A**) Percentage of donor-derived cells (CD45.1$^+$) in total PB leukocytes or myeloid cell (Mac1$^+$), B lymphocyte (B220$^+$), and T lymphocyte (CD3$^+$) fractions 1 to 4 months after secondary BM transplantation. Data represent means ± SEM from 20 to 22 mice per group. (**B** and **C**) Cumulative HSC proliferation after a single dose of 5-FU ± G1T28 treatment as determined by H2B-GFP label retention 4 weeks after 5-FU administration. Representative H2B-GFP label dilution histograms (and curve fitting) are shown in (B), with quantification in (C). PI indicates the average number of daughter cells generated from a single, originally labeled HSC by the time of analysis, such that $\log_2$ (PI) equals the average number of HSC divisions. Data represent means ± SD from 3 to 6 mice in three experiments. Statistical significance was assessed by unpaired two-tailed Student's t test (*P < 0.05, **P < 0.01, ***P < 0.001). div, division.

An analysis of the BM of recipient mice at 32 weeks after transplantation showed that G1T28 pretreatment also increased donor cell reconstitution of all lineages in the BM compared to 5-FU treatment alone (Fig. 4F). Analogous to transplantation studies comparing murine HSCs from young and old donors (*31*, *35*, *36*), the frequency of donor-derived HSCs in recipient BM was not reduced by 5-FU treatment, regardless of G1T28 administration (Fig. 4F). These findings indicate that a period of G_1 arrest bracketing the time of each 5-FU treatment rescues HSC exhaustion—a decline in HSC function on a per-cell basis that is induced by serial exposure to chemotherapy or aging.

To determine the durability of HSC protection afforded by G1T28-induced G_1 arrest, we transplanted 10^7 total BM cells from each primary recipient into lethally irradiated individual secondary recipient mice 32 weeks after the initial transplantation. HSCs from G1T28-treated mice continued to produce significantly greater overall reconstitution in the secondary recipients (Fig. 5A; P < 0.05). Notably, although BM cells treated with 5-FU only contributed poorly to PB lymphoid cells in secondary recipients (Fig. 5A), consistent with the myeloid-skewed differentiation pattern of aged or exhausted HSCs (*31*, *37*), G1T28-pretreated cells maintained robust lymphoid reconstitution potential (Fig. 5A). Accordingly, when a separate group of 5-FU ± G1T28–treated mice were analyzed 13 months after the fourth dose of 5-FU (in the absence of BM transplantation), G1T28-pretreated mice also showed a significantly higher PB lymphoid–to–myeloid cell ratio compared to 5-FU–only–treated mice (fig. S9D; P < 0.05). We carefully monitored our colonies for malignancy after primary and secondary transplantation but did not observe the emergence of secondary hematologic malignancies in any 5-FU ± G1T28–treated mice or BM transplant recipients during a 1-year follow-up period. Together, these results indicate that PQ at the time of serial 5-FU treatment protects the long-term reconstitution potential of HSCs

and attenuates the myeloid-biased differentiation of damaged or aged HSCs.

G1T28-induced G_1 arrest protects long-term HSC function against serial 5-FU treatment by reducing HSC proliferative burden

To directly demonstrate that transient G_1 arrest attenuates HSC exhaustion through a reduction in proliferative burden, we analyzed the proliferative history of individual HSCs after a single dose of 5-FU with or without G1T28 pretreatment using the histone H2B–green fluorescent protein (H2B-GFP) label dilution assay (*38*, *39*). In this assay, the replicative history of an individual HSC can be inferred by measuring the dilution of GFP-tagged histones, which are conditionally expressed under the control of a doxycycline-inducible promoter. Specifically, adult *H2B-GFP;M2-rtTA* double-transgenic mice were treated with doxycycline for 6 weeks to label all HSCs with H2B-GFP (*39*). Two weeks after doxycycline removal, mice received vehicle, G1T28, 5-FU, or 5-FU + G1T28 (with G1T28 given 12 hours before 5-FU). H2B-GFP expression in BM HSCs was quantified 4 weeks after 5-FU treatment, allowing time for complete hematologic recovery. In mice that received vehicle only, BM HSCs divided 2.1 ± 0.4 times on average, generating 4.3 ± 2.1 daughter HSCs [or a proliferation index (PI) of 4.3 ± 2.1] over the 6 weeks after doxycycline removal (Fig. 5B). G1T28 treatment alone did not affect HSC proliferation over the same period (2.4 ± 1.0 divisions; PI, 6.2 ± 2.6) (Fig. 5, B and C). In contrast, a single injection of 5-FU greatly increased HSC proliferation (5.3 ± 0.5 divisions; PI, 41.3 ± 5.4), which was partially rescued by G1T28 pretreatment (4.6 ± 0.4 divisions; PI, 25.2 ± 4.7) (Fig. 5, B and C). Notably, this benefit was observed after only a single round of 5-FU. We were unable to assess the entire proliferation history of individual HSCs after four rounds of 5-FU treatment because of detection limitations of the H2B-GFP label dilution assay, but we expect that the benefit of PQ would be cumulative with additional cycles. Therefore, PQ at the time of 5-FU treatment appears to attenuate HSC exhaustion, at least in part, by reducing the number of proliferative events inflicted on an HSC by each round of chemotherapy.

DISCUSSION

Here, we have shown that G1T28, a potent and selective CDK4/6i, can induce a specific and transient G_1 cell cycle inhibition in HSPCs, particularly HSCs. In accord with previous works (*17*, *18*), a transient G_1 arrest induced by contemporaneous administration of this CDK4/6i at the time of chemotherapy can markedly ameliorate the acute hematopoietic toxicity of cytotoxic chemotherapy. Notably, we showed that in addition to a beneficial effect on rapidly proliferating hematopoietic progenitors, PQ can also provide lasting protection of the per-cell function of quiescent HSCs, thereby ameliorating the long-term toxicity associated with serial exposure to chemotherapy agents ("exhaustion").

We also describe first-in-human results of G1T28 in a phase 1 trial in healthy volunteers, showing that G1T28 has minimal toxicity and excellent PK and induces a strong proliferative arrest of early human HSPCs. G1T28 is well tolerated after a single intravenous infusion and has robust PD activity in the BM. At the BED of 192 mg/m^2, BM HSPCs exhibited robust G_1 cell cycle arrest at 24 and 32 hours after treatment, which should be a sufficient length of time to maintain HSPC quiescence when coadministered with chemotherapy. Standard-of-care chemotherapy for small-cell lung cancer (SCLC) includes carboplatin and etoposide in the first-line setting and single-agent topotecan in the second-/third-line setting. Terminal half-lives for these agents are 6, 7.5, and 3 hours, respectively. On the basis of these half-lives, a 32-hour G_1 arrest would allow about 94% (four half-lives) of the etoposide to be cleared and even more for the other agents. The desired characteristics for a CDK4/6i used for chemoprotection differ from those developed as antineoplastic agents, where typical properties tend to include a longer biological half-life that supports single daily dosing, large volume of distribution, accumulation on repeated dosing, and oral delivery. As expected, considering the dependence of early HSPCs on CDK4/6 for proliferation, continued daily administration of antineoplastic CDK4/6is is associated with myelosuppression, particularly neutropenia (*40*, *41*). It is believed that this is not a cytotoxic effect on the HSPCs but a mechanism-based result of continued blockade of HSPC proliferation that decreases the production of new blood cells. In contrast, we have shown that a brief and transient period of CDK4/6 inhibition by G1T28 does not have lingering myelosuppressive effect.

The current study extends earlier work on chemotherapy-induced acute myelosuppression (*17*) by showing beneficial effects after multiple cycles of chemotherapy treatment that are long-lasting, transplantable, and associated with enhanced HSC function. Unlike lineage-specific strategies used in the clinic to manage acute chemotherapy–induced myelosuppression (such as transfusions and G-CSF/EPO), CDK4/6i-induced PQ protects all blood cell lineages. Moreover, unlike growth factor treatment, which enhances short-term blood cell count recovery at the cost of increasing the risk of leukemia and BM failure (*6*–*9*), a CDK4/6i-induced G_1 arrest coincident with chemotherapy administration preserves HSC function. Therefore, CDK4/6i-mediated PQ provides the additional benefit of ameliorating the long-term sequelae of cytotoxic agents.

Chemotherapy-associated late BM toxicity results from therapy-induced damage and premature exhaustion of HSCs. Cytotoxics not only can cause direct damage to activated HSCs but also can induce functional attrition of HSCs indirectly through a process of proliferative exhaustion (Figs. 4 and 5) (*22*). This HSC-intrinsic damage leads to a reduction of long-term multilineage reconstitution potential, as well as myeloid-biased differentiation. Reduced long-term HSC function is clinically manifested in cancer survivors as persistent cytopenias, high rates of secondary leukemia and MDS, reduced T cell production, and decreased cellular immunity. Here, we showed that PQ can attenuate chemotherapy-induced HSC exhaustion and lineage bias by directly modulating the cell cycle of rapidly proliferating activated HSCs at the time of exposure to cytotoxic agents, as well as by indirectly protecting quiescent HSCs by reducing their proliferative burden. Although we were unable to directly assess the effect of CDK4/6 inhibition on the incidence of chemotherapy-induced secondary leukemia, we provide evidence that a G1T28-induced G_1 arrest will attenuate most aspects of chemotherapy-induced late BM toxicity.

Beyond reducing late toxicity, the preservation of HSC function would be expected to increase rates of tumor response and long-term cure through a variety of mechanisms. First, dose density and intensity are important predictors of tumor response in several RB-deficient tumors [such as SCLC (*42*) and triple-negative breast cancer (TNBC) (*43*)], and reduced HSC exhaustion would prevent the dose reductions and treatment delays mandated by the persistent cytopenias that commonly occur in patients after multiple cycles of therapy. Moreover, by reducing HSC myeloid bias and thereby preserving T cell production, this approach could be "immune-sparing." An extensive clinical literature suggests that treatment-related lymphopenia is associated with

worsened outcome in several types of cancer (*44*). A preservation of cellular immunity could be especially important in patients who will later receive immune checkpoint inhibitors that induce antitumor immunity through the activation of T cells.

A limitation of the PQ approach is that a CDK4/6i-induced G_1 arrest at the time of chemotherapy administration could protect tumor cells in addition to normal HSPCs (*11*, *16*). Therefore, it will be important to limit this approach to patients whose cancer proliferates independently of CDK4/6 activity. However, note that CDK4/6-independent cancers are not rare: It is estimated in the United States alone that there are 300,000 new cases of cancers annually whose proliferation does not depend on CDK4/6 activity (*16*). Several molecular lesions would be expected to render a cancer CDK4/6-independent, the best described of which is inactivation of the RB protein (*15*, *17*, *45*, *46*). *RB1* is genetically inactivated in ~11% of human cancers (*15*), including virtually 100% of SCLCs (*47*) and at high frequency in TNBCs (*48*), as well as advanced carcinomas of the prostate (*49*) and bladder (*50*). Likewise, functional inactivation of RB through expression of the E7 oncoprotein of human papillomavirus is common in squamous malignancies of the head and neck, anus, and cervix (*51*). Finally, we believe that an even larger fraction of cancers that retain RB expression are functionally deficient in RB through high-level activation of CDK2, which phosphorylates RB, by mechanisms that do not depend on CDK4/6 activity. For example, direct cyclin E amplification has been reported at moderate frequency (>20%) in several human solid tumors (TNBC, ovarian carcinoma, advanced prostate, and bladder cancer) (*52*). Further evidence for this notion comes from the Novartis Cell Line Encyclopedia screens, which have shown that the vast majority of RB-expressing human cell lines are highly resistant to palbociclib (EC_{50} > 2 μM) and therefore likely to be CDK4/6-independent (*15*). Therefore, although CDK4/6i-mediated protection of normal HSPCs will not benefit all cancer patients, it offers a potential means to address debilitating short- and long-term side effects of cytotoxic chemotherapy in a large number of patients with CDK4/6-independent cancer.

Another limitation of this work is the schedule-dependent nature of this approach. We have shown that optimal protection is achieved when the period of HSPC G_1 arrest overlaps with the in vivo biological effects of chemotherapy, but not for a longer or shorter period. If the period of growth arrest is too short, HSPCs reenter the cell cycle in the setting of unrepaired DNA damage, causing increased myelosuppression. Likewise, an overly long period of PQ prolongs count nadirs after chemotherapy. Therefore, the safe use of this approach in patients requires the careful timing of HSPC arrest relative to the effective half-life of the chemotherapy agents. These concerns can be largely addressed through the use of an agent-like G1T28, with an intravenous formulation and a relatively short pharmacologic half-life, allowing for precise control of the period of HSPC cycle arrest.

In summary, we have shown precise control of human and murine HSPC proliferation using a small-molecule CDK4/6i, G1T28. By using this agent to induce a transient cell cycle arrest at the time of exposure to cytotoxics, we have shown long-lasting and cell-intrinsic protection of murine HSCs from chemotherapy-induced exhaustion. We also demonstrated that G1T28 is well tolerated after intravenous administration in healthy human volunteers and has robust PD activity in inducing transient and reversible cell cycle arrest of BM HSPCs, suggesting that CDK4/6i-induced PQ is feasible in humans. Because G1T28 is currently undergoing testing in this fashion in patients with SCLC (NCT02499770 and NCT02514447) and metastatic TNBC (NCT02978716), it will be possible to determine whether PQ similarly benefits human HSCs. Such an effect would be expected to increase chemotherapy efficacy and reduce late toxicity such as secondary leukemia and MDS in a large fraction of patients receiving cytotoxic chemotherapy.

MATERIALS AND METHODS

Study design

The preclinical portion of the current study aimed to determine whether transient G_1 cell cycle arrest induced by pharmacological CDK4/6 inhibition could attenuate the late hematopoietic toxicity of cytotoxic chemotherapy. The well-characterized murine model of 5-FU–induced myelosuppression was used to assess the BM protective effect of G1T28. The effect of G1T28 on 5-FU–induced HSC exhaustion was assessed by a variety of approaches including serial competitive BM transplantation. The data presented in this study reflect multiple independent experiments performed on separate days using different mice and contain more than three biological replicates. No statistical methods were used to predetermine the sample size. No data or outliers were excluded from our analyses. Age- and gender-matched mice were randomly treated with vehicle or the test compounds, and lethally irradiated mice were randomly assigned as BM transplantation recipients of variously treated donors. The investigators were not blinded during sample allocation or result analysis. The end point for the survival assay was determined as loss of more than 20% of peak body weight and/or deterioration of body condition. The extent of PB donor chimerism in BM transplantation recipients was monitored for more than 16 weeks to assess long-term multilineage reconstitution potential.

The clinical portion of the current study aimed to assess the safety, PK, and PD of intravenously administered G1T28 in healthy human volunteers. It was designed as a single-center, single-dose first-in-human study (NCT02243150), including a double-blind, randomized, placebo-controlled (3:1 G1T28 versus placebo administered as a 30-min intravenous infusion) SAD part in six four- to eight-subject cohorts, and an open-label 12-subject cohort to confirm the BED. The study followed a Continual Reassessment Method design, informed by the accrued safety experience throughout the study. Dose escalation between cohorts and the expansion from four- to eight-subject cohorts were determined by the Safety Monitoring Committee (SMC) based on available safety, PK, and PD data. Up to a 100% dose escalation was allowed between cohorts, if supported by the available safety, PK, and PD data. Dose escalation was planned to continue until the SMC deemed that the BED had been reached or the criteria for halting dose escalation had been met. Dose escalation was to be halted in the following situations: occurrence of drug-related treatment emergent ≥grade 2 nonhematologic AEs or ≥grade 3 hematologic AEs in two or more subjects in a given cohort, occurrence of drug-related treatment emergent ≥grade 3 nonhematologic AEs or ≥grade 4 hematologic AEs in a single subject in a given cohort, or a recommendation to halt dose escalation provided by the principal investigator. On the basis of preclinical PK/PD modeling and available safety, PK, and PD data from cohorts 1 to 6, 12 subjects were enrolled in cohort 7 to confirm the BED. All 12 subjects enrolled in cohort 7 had a single BM aspirate obtained at various time points relative to intravenous dosing of G1T28 to directly measure the effect of G1T28 on BM HSPC proliferation. The protocol and informed consent were reviewed and approved by the Institutional Independent Ethics Committee, and the trial was conducted in accordance with the principles of the Declaration of Helsinki, in compliance with the International Conference on Harmonization E6 Guideline for Good Clinical Practice and the

European Union Clinical Trial Directive. All subjects provided written informed consent.

Mice

Mice used in this study were housed in the Association for Assessment and Accreditation of Laboratory Animal Care–accredited, specific pathogen–free animal care facility operated by the Division of Laboratory Animal Medicine at the University of North Carolina (UNC) at Chapel Hill. Mouse work was conducted in accordance with protocols approved by the Institutional Animal Care and Use Committee. C57BL/6NTac (CD45.2) and B6.SJL-*Ptprc*^{a}/BoyAiTac (CD45.1) mice were purchased from Taconic. B6;129S4-*Gt(ROSA)26Sor*$^{tm1(rtTA*M2)Jae}$*Col1a1*$^{tm7(tetO\text{-}HIST1H2BJ/GFP)Jae}$/J (*H2B-GFP;M2-rtTA*) double-transgenic mice were purchased from the Jackson Laboratory.

Cell isolation and flow cytometry

Murine BM cells were isolated by flushing the femurs, tibias, and pelvic bones using ice-cold staining medium [1× Ca^{2+}- and Mg^{2+}-free Hanks' balanced salt solution (Gibco) supplemented with 10 mM EDTA (Corning) and 2% heat-inactivated bovine serum (Gibco)] and filtered through 40-μm nylon mesh (Sefar). Splenocytes and thymocytes were isolated by crushing spleen or thymus tissue between two microscope slides followed by filtering through nylon mesh. The number of viable cells was determined by manually counting with a hemocytometer. To identify HSCs, LSK cells, and MPs by flow cytometry, BM cells were stained with antibodies against c-Kit [2B8, allophycocyanin (APC)–eFluor 780; eBioscience], Sca-1 (E13-161.7, APC), CD48 [HM48-1, peridinin chlorophyll protein (PerCP)–Cy5.5], CD150 (TC15-12F12.2, Biotin), as well as fluorescein isothiocyanate (FITC)–conjugated antibodies against the following lineage markers: CD2 (RM2-5), CD3e (145-2c11), CD4 (GK1.5), CD5 (53-7.3), CD8a (53-6.7), B220 (RA3-6B2), Mac-1 (M1/70), Gr-1 (RB6-8C5), and Ter119 (TER-119). CD150 staining was developed using phycoerythrin (PE)–Cy7–conjugated streptavidin. Sometimes, c-Kit–expressing cells were magnetically enriched using anti-APC magnetic beads on the autoMACS system (Miltenyi). To identify mature myeloid, erythroid, and B lineage cells, BM cells were stained with antibodies against Gr-1 (FITC), B220 (PerCP-Cy5.5), Ter119 (Alexa Fluor 700), and Mac-1 (APC–eFluor 780, eBioscience). All antibody staining of live cells was carried out on ice for 1 hour. All primary and secondary antibodies were purchased from BioLegend unless otherwise indicated. Flow cytometry analysis of stained cells was performed on a customized LSR II seven-laser, 17-color flow cytometer (Becton Dickinson), and recorded data were analyzed in BD FACSDiva 8.0.1, FlowJo 10.0.8, or FCS Express 5 Pro RUO software.

Murine HSPC cycle analysis by EdU incorporation assay

EdU-labeled murine BM cells and thymocytes were isolated and stained with primary antibodies as described above. The stained cells were then labeled with LIVE/DEAD Fixable Red Dead Cell Stain (Life Technologies) for 30 min, followed by fixation in 5% formalin on ice for 10 min and permeabilization in staining medium plus 0.1% saponin for 10 min at room temperature. EdU staining was performed in 0.1 M tris-HCl (pH 7.5), 1 mM $CuSO_4$, 0.1 M ascorbic acid, and 5 μM Alexa Fluor 555 azide (Life Technologies) for 10 min at room temperature (*53*). Stained cells were washed twice with ice-cold staining medium, followed by incubation in secondary antibody and 4′,6-diamidino-2-phenylindole (2 μg/ml) for 30 min on ice before flow cytometry analysis.

In vivo G1T28 murine PK assay

For PK study after intraperitoneal administration, 4- to 5-month-old female C57BL/6NHsd mice were given a single injection of 50 or 100 mg/kg of G1T28. For oral PK study, 8- to 10-week-old male CD1 mice were gavaged with 10, 50, or 100 mg/kg of G1T28. Blood was collected from treated mice via cardiac puncture at 5, 15, and 30 min or 1, 2, 4, 8, 12, 18, 24, 36, and 48 hours after drug administration (three mice per dose per time point). Plasma G1T28 concentration was determined by liquid chromatography–tandem mass spectrometry (LC-MS/MS) as follows. Murine plasma samples were spiked with G1T28 and the corresponding D3 stable label internal standard (IS), followed by protein precipitation with acetonitrile. After precipitation, a portion of the organic layer was transferred to a 96-well plate, and the extract was chromatographed by reversed-phase high-performance liquid chromatography (HPLC) on an Allure PFP Propyl column with a mobile phase containing acetonitrile, water, ammonium formate, and formic acid. G1T28 and D3 IS were detected by monitoring the precursor and product ions [mass/charge ratio (*m*/*z*), 447.2 and 336.2 for G1T28; *m*/*z*, 450.2 and 339.4 for G1T28 D3 IS) with a Sciex 4000 LC-MS/MS system. Analyte-to-IS peak area ratios for the standards were used to create linear calibration curves with weighted ($1/x^2$) least squares regression analysis. The calibration range of the assay was 10 to 10,000 ng/ml with a sample volume of 20 μl of plasma. PK parameters on plasma G1T28 concentration were calculated in Watson (v7.3.0.01, Thermo Inc.).

In vivo G1T28 dose response and PD assay

To determine the dose response of various murine hematopoietic cell types to G1T28-induced cell cycle arrest, 8- to 10-week-old female C57BL/6 mice were treated with a single dose of 0, 10, 25, 50, 100, or 150 mg/kg of G1T28 by intraperitoneal injection. Twelve hours later, each mouse was given a single intraperitoneal injection of EdU (10 mg/kg) and harvested 2 hours later. EdU staining of BM cells and thymocytes was performed as described above. To determine the in vivo PD of G1T28 on murine hematopoietic cell proliferation, 8- to 10-week-old female C57BL/6 mice were given a single intraperitoneal injection of 50 or 100 mg/kg of G1T28, followed by a single intraperitoneal injection of EdU (10 mg/kg) at 0.5, 1, 2, 4, 6, 12, 18, 24, 36, 48, 72, or 168 hours later. BM cells and thymocytes were isolated 2 hours after EdU injection and stained as described above. To determine the effect of G1T28 on actively cycling HSCs, 8-week-old female C57BL/6 mice were given a single intraperitoneal injection of 5-FU (150 mg/kg). Four days later, half (n = 4) of the treated mice received a single intraperitoneal injection of G1T28 (100 mg/kg), and the other half (n = 4) received vehicle (50 mM citrate buffer) solution. Twelve hours later, each mouse was labeled with EdU for 2 hours. The frequency of EdU^+ HSCs in each treatment group was determined as described.

5-FU survival assay

Eight- to 10-week-old female C57BL/6 mice were given a single intraperitoneal injection of 5-FU (150 mg/kg) once every 7 or 10 days. G1T28 was given to a subset of 5-FU–treated animals at 30 min, 12 hours, and/or 24 hours before each 5-FU treatment at 50 or 100 mg/kg dose by intraperitoneal injection. Pegfilgrastim (250 μg/kg) was given to a subset of 5-FU–treated animals 24 hours after each 5-FU treatment by subcutaneous injection. Treated mice were monitored daily for body condition and/or weight loss, and the end point was determined as severe deterioration of body condition and/or loss of more than 20% of peak body weight.

Methylcellulose colony formation assay

C57BL/6 mice were orally gavaged with vehicle or G1T28 (150 mg/kg) 30 min or 12 hours before being treated with 5-FU (150 mg/kg). BM progenitor colony formation assay was performed by plating 1×10^4, 3×10^4, or 6×10^4 unfractionated BM cells harvested at 1, 2, or 4 days after 5-FU into methylcellulose culture medium (MethoCult GF M3434; STEMCELL Technologies). Hematopoietic colonies were counted after 8 to 9 days of culture at 37°C in 5% CO_2.

Serial 5-FU treatment and competitive BM reconstitution assay

Eight-week-old female B6.SJL-*Ptprc*^{a}/BoyAiTac (CD45.1) mice were treated with four rounds of vehicle [1× phosphate-buffered saline (PBS)] or 5-FU (150 mg/kg) at 3-week intervals. A subset of the 5-FU–treated mice was given a single dose of G1T28 (150 mg/kg) by oral gavage 30 min before each 5-FU injection or two doses of pegfilgrastim (250 μg/kg) by subcutaneous injection at 24 and 48 hours after each 5-FU treatment, and the remaining mice received vehicle [50 mM citrate buffer (pH 4.0) for gavaging and 0.1% bovine serum albumin in 1× PBS for subcutaneous injection] treatment. CBCs were analyzed 4, 7, 11, 14, 18, and 21 days after the last round of 5-FU treatment to assess the rate of hematologic recovery. Eight weeks after the last dose of 5-FU treatment, BM cells were harvested from the treated mice, and competitive long-term BM reconstitution assay was performed by transplanting 500,000 total BM cells (CD45.1$^+$) from each donor, together with 500,000 competitor BM cells (CD45.2$^+$, from 8-week-old C57BL/6 mice), into lethally irradiated 8-week-old female C57BL/6 (CD45.2$^+$) recipients. Lethal irradiation was carried out using a Gammacell 40 Exactor Cesium-137 γ-ray source (MDS Nordia) by giving two doses of 540 rads total body irradiation 2 hours apart. BM cells from each donor mouse were transplanted into five recipient mice, and five donors were transplanted from each treatment group. PB was collected from the tail veins of recipient mice at 4-week intervals for at least 16 weeks after transplantation. To assess the frequency of donor cells in PB, red blood cells were subjected to ammonium-chloride-potassium lysis (*54*), and the remaining leukocytes were stained with antibodies against CD45.2 (104, FITC), CD45.1 (A20, APC–eFluor 780, eBioscience), B220 (PerCP-Cy5.5), Mac-1 (APC), CD3e (PE), and Gr-1 (PE-Cy7). Thirty-two weeks after initial transplantation, BM cells were harvested from each primary recipient mouse and analyzed for donor cell contribution to each hematopoietic lineage. For HSC analysis, BM cells were stained with antibodies against lineage markers (FITC), c-Kit (APC–eFluor 780), Sca-1 (PE-Cy7), CD150 (PerCP-Cy5.5), CD48 (PE), CD45.1 (BV421), and CD45.2 (Biotin, followed by streptavidin–Alexa Fluor 647). For analysis of mature myeloid, B, and T cells, BM cells were stained with antibodies against Mac-1 (APC–eFluor 780), Gr-1 (PE-Cy7), B220 (PerCP-Cy5.5), CD3 (PE), CD45.2 (FITC), and CD45.1 (BV421). Secondary BM transplantation was performed by transplanting 1×10^7 total BM cells from each primary recipient into an individual lethally irradiated secondary recipient (CD45.2$^+$). The frequencies of donor CD45.1$^+$ cells in each blood lineage were monitored by analyzing the PB of secondary recipients at 4-week intervals for at least 16 weeks after transplantation.

H2B-GFP label dilution assay

To analyze the proliferation history of HSCs after 5-FU and/or G1T28 treatment, adult homozygous *H2B-GFP;M2rtTA* mice were treated with doxycycline (2 mg/ml) in drinking water for 6 weeks to label all HSCs. Two weeks after removing doxycycline, mice were given a single dose of vehicle or G1T28 (150 mg/kg) by oral gavage 12 hours before vehicle or 5-FU (150 mg/kg) treatment. Four weeks after 5-FU administration, BM cells were harvested and analyzed for H2B-GFP expression. Unfractionated BM cells were stained with antibodies against lineage markers (Biotin, followed by streptavidin–PE-Cy7), CD150 (PE), CD48 (PerCP-Cy5.5), c-Kit (APC–eFluor 780), and Sca-1 (APC). Curve fitting for HSC H2B-GFP label dilution data was performed using the proliferation analysis module in FCS Express 5 Pro RUO software.

Human study population and safety assessment

Eligible subjects included males and females 18 to 60 years of age with a BMI of 18 to 32 kg/m^2 (inclusive) and a weight of at least 50 kg. The subjects had to be judged to be in good health on the basis of medical history and physical examination including vital signs, ECG, and clinical laboratory results. Women of childbearing potential were determined to be in a nongravid state and had agreed to take appropriate precautions to avoid pregnancy from the study enrollment until 3 months after completion of the study. Male subjects with a female partner of childbearing potential were required to use a highly effective form of birth control during the study and for 3 months after completion of the study. Use of medications or herbal products within 14 days before the start of the study was not allowed. Use of investigational medications within 60 days of the start of the study was not allowed.

Safety and tolerability assessments consisted of monitoring AEs, clinical laboratory results, vital signs, 12-lead ECGs, and physical examination. Subjects were admitted to the clinic on day −1 and remained in the clinic until all study procedures had been completed on day 5. Subjects returned to the clinic for further evaluation on days 7, 10, and 14. The reporting period for serious AEs began from the time that the subject provided informed consent up to and including the day 14 follow-up visit. AEs were recorded from the time of first dosing up to and including the day 14 follow-up visit, and all AEs had to be followed up until they had resolved, returned to baseline, or was deemed that further recovery was unlikely. Toxicity was assessed using the National Cancer Institute (NCI) Common Terminology Criteria for Adverse Events v4.0 criteria.

Human PK study

G1T28 concentration in human plasma and urine was determined using a validated LC-MS/MS assay. For assay validation, human plasma samples were spiked with G1T28 and the corresponding D3 stable label IS, followed by protein precipitation using acetonitrile. A portion of the organic layer after protein precipitation was transferred to a 96-well plate, and the extract was chromatographed by reversed-phase HPLC on a Waters XBridge C18 (part no.186003021) with a mobile phase containing acetonitrile, water, ammonium acetate, and formic acid. G1T28 and the D3 IS were detected by monitoring the precursor and product ions (m/z, 447 and 336 for G1T28; m/z, 450 and 339 for G1T28 D3 IS) with a Sciex API 4000 LC-MS/MS system. Analyte-to-IS peak area ratios for the standards were used to create linear calibration curves with weighted ($1/x^2$) least squares regression analysis. The calibration range of the assay was 0.5 to 1000 ng/ml, with a sample volume of 50 μl of plasma. The precision, accuracy, selectivity, and lower limit of quantification of the assay were determined for G1T28, and the benchtop, freeze/thaw, and freezer stability of the analyte under the conditions of the assay were determined with appropriate quality control samples. All of the assessments met the acceptance criteria established for a validated assay. Using this validated

assay, plasma (cohorts 1 to 7) and urine (cohort 7) concentrations of G1T28 were determined with lower limits of quantitation of 0.5 and 5.0 ng/ml in plasma and urine, respectively. Blood samples were collected before the dose and at multiple time points after the dose. Standard PK parameters were calculated using both a noncompartmental and a compartmental method (Phoenix WinNonlin 6.3).

Human BM proliferation assay

A single BM aspirate was obtained from all subjects enrolled in the BED cohort (cohort 7, 192 mg/m^2; n = 12) to determine the effect of G1T28 on the percentage of various BM progenitor lineages in the G_0-G_1 or S-G_2-M phases of the cell cycle. Using flow cytometry, lineages were identified using the markers CD45, CD34, CD14, CD11b, CD71, and CD61, and the cell cycle phases were evaluated using DRAQ5 DNA dye. BM progenitor cell proliferation was measured before dosing (n = 5), 24 hours after G1T28 dosing (n = 3), or 32 hours after G1T28 dosing (n = 4). Two BM samples (one before a dose and one at 32 hours after a dose) were heavily contaminated with PB, were considered technically inadequate, and were removed from the cell cycle analysis data sets.

Statistical analysis

Statistical significance of differences between two sample groups was assessed using two-tailed Student's t test in GraphPad Prism 6 after the similarities in data variance between groups were determined using F test. The survival analysis of mice after serial 5-FU treatment was performed in GraphPad Prism 6 using log-rank test. Sample sizes for all data are given in each figure legend. Error bars represent SEM or SD as described in the figure legends. Unless otherwise indicated, a P value of <0.05 was considered statistically significant.

Demographic and safety data for each human subject were tabulated and summarized using descriptive statistics. Summary statistics (means, minimum-maximum, SDs, and coefficients of variation) were calculated using noncompartmental and compartmental methods with WinNonlin software (v6.3, Pharsight) for the concentration versus time data at each sampling and for derived PK parameters. Comparisons of the proliferation of various human hematopoietic stem and progenitor subsets at baseline or after G1T28 treatment were made using two-tailed t test with a P value of 0.05.

SUPPLEMENTARY MATERIALS

www.sciencetranslationalmedicine.org/cgi/content/full/9/387/eaal3986/DC1

Fig. S1. Flow cytometry gating strategy for various murine BM hematopoietic lineages.
Fig. S2. Representative flow cytometry plots for EdU staining in indicated murine hematopoietic cell types.
Fig. S3. Dose-dependent G_1 cell cycle arrest induced by G1T28 in a wide range of murine hematopoietic cell types.
Fig. S4. Transient and reversible cell cycle arrest induced by G1T28 in murine hematopoietic cells.
Fig. S5. In vivo PK of G1T28 after intraperitoneal or oral administration in mice.
Fig. S6. Flow cytometry gating strategy for various human BM hematopoietic lineages.
Fig. S7. Cell cycle analysis of human BM hematopoietic progenitors at various time points after a single dose of G1T28.
Fig. S8. Changes in PB cell counts in human subjects after a single dose of G1T28.
Fig. S9. Accelerated hematologic recovery by G1T28 pretreatment after serial 5-FU treatment.
Table S1. Summary of demographic characteristics of healthy volunteers.
Table S2. Summary of G1T28 administration in human subjects.
Table S3. Summary of related TEAEs reported in ≥10% of subjects.
Table S4. Summary of plasma G1T28 PK parameters in humans.
Table S5. Absolute frequencies of human BM lineage populations in G_0-G_1 or S-G_2-M phases of the cell cycle after G1T28 administration.
Table S6. Median survival extension by CDK4/6i or pegfilgrastim in mice receiving serial 5-FU treatment.

REFERENCES AND NOTES

1. J. Harris, D. Sengar, T. Stewart, D. Hyslop, The effect of immunosuppressive chemotherapy on immune function in patients with malignant disease. *Cancer* **37**, 1058–1069 (1976).
2. R. V. Gardner, C. Lerner, C. M. Astle, D. E. Harrison, Assessing permanent damage to primitive hematopoietic stem cells after chemotherapy using the competitive repopulation assay. *Cancer Chemother. Pharmacol.* **32**, 450–454 (1993).
3. P. Mauch, L. Constine, J. Greenberger, W. Knospe, J. Sullivan, J. L. Liesveld, H. J. Deeg, Hematopoietic stem cell compartment: Acute and late effects of radiation therapy and chemotherapy. *Int. J. Radiat. Oncol. Biol. Phys.* **31**, 1319–1339 (1995).
4. R. V. Gardner, Long term hematopoietic damage after chemotherapy and cytokine. *Front. Biosci.* **4**, e47–e57 (1999).
5. Y. Wang, V. Probin, D. Zhou, Cancer therapy-induced residual bone marrow injury: Mechanisms of induction and implication for therapy. *Curr. Cancer Ther. Rev.* **2**, 271–279 (2006).
6. R. L. Hornung, D. L. Longo, Hematopoietic stem cell depletion by restorative growth factor regimens during repeated high-dose cyclophosphamide therapy. *Blood* **80**, 77–83 (1992).
7. M. A. Moore, Does stem cell exhaustion result from combining hematopoietic growth factors with chemotherapy? If so, how do we prevent it? *Blood* **80**, 3–7 (1992).
8. D. Hershman, A. I. Neugut, J. S. Jacobson, J. Wang, W.-Y. Tsai, R. McBride, C. L. Bennett, V. R. Grann, Acute myeloid leukemia or myelodysplastic syndrome following use of granulocyte colony-stimulating factors during breast cancer adjuvant chemotherapy. *J. Natl. Cancer Inst.* **99**, 196–205 (2007).
9. G. H. Lyman, D. C. Dale, D. A. Wolff, E. Culakova, M. S. Poniewierski, N. M. Kuderer, J. Crawford, Acute myeloid leukemia or myelodysplastic syndrome in randomized controlled clinical trials of cancer chemotherapy with granulocyte colony-stimulating factor: A systematic review. *J. Clin. Oncol.* **28**, 2914–2924 (2010).
10. M. Tubiana, P. Carde, E. Frindel, Ways of minimising hematopoietic damage induced by radiation and cytostatic drugs—The possible role of inhibitors. *Radiother. Oncol.* **29**, 1–17 (1993).
11. M. V. Blagosklonny, A. B. Pardee, Exploiting cancer cell cycling for selective protection of normal cells. *Cancer Res.* **61**, 4301–4305 (2001).
12. M. Malumbres, R. Sotillo, D. Santamaria, J. Galán, A. Cerezo, S. Ortega, P. Dubus, M. Barbacid, Mammalian cells cycle without the D-type cyclin-dependent kinases Cdk4 and Cdk6. *Cell* **118**, 493–504 (2004).
13. K. Kozar, M. A. Ciemerych, V. I. Rebel, H. Shigematsu, A. Zagozdzon, E. Sicinska, Y. Geng, Q. Yu, S. Bhattacharya, R. T. Bronson, K. Akashi, P. Sicinski, Mouse development and cell proliferation in the absence of D-cyclins. *Cell* **118**, 477–491 (2004).
14. S. M. Johnson, C. D. Torrice, J. F. Bell, K. B. Monahan, Q. Jiang, Y. Wang, M. R. Ramsey, J. Jin, K.-K. Wong, L. Su, D. Zhou, N. E. Sharpless, Mitigation of hematologic radiation toxicity in mice through pharmacological quiescence induced by CDK4/6 inhibition. *J. Clin. Invest.* **120**, 2528–2536 (2010).
15. M. J. Garnett, E. J. Edelman, S. J. Heidorn, C. D. Greenman, A. Dastur, K. W. Lau, P. Greninger, I. R. Thompson, X. Luo, J. Soares, Q. Liu, F. Iorio, D. Surdez, L. Chen, R. J. Milano, G. R. Bignell, A. T. Tam, H. Davies, J. A. Stevenson, S. Barthorpe, S. R. Lutz, F. Kogera, K. Lawrence, A. McLaren-Douglas, X. Mitropoulos, T. Mironenko, H. Thi, L. Richardson, W. Zhou, F. Jewitt, T. Zhang, P. O'Brien, J. L. Boisvert, S. Price, W. Hur, W. Yang, X. Deng, A. Butler, H. G. Choi, J. W. Chang, J. Baselga, I. Stamenkovic, J. A. Engelman, S. V. Sharma, O. Delattre, J. Saez-Rodriguez, N. S. Gray, J. Settleman, P. A. Futreal, D. A. Haber, M. R. Stratton, S. Ramaswamy, U. McDermott, C. H. Benes, Systematic identification of genomic markers of drug sensitivity in cancer cells. *Nature* **483**, 570–575 (2012).
16. U. Asghar, A. K. Witkiewicz, N. C. Turner, E. S. Knudsen, The history and future of targeting cyclin-dependent kinases in cancer therapy. *Nat. Rev. Drug Discov.* **14**, 130–146 (2015).
17. P. J. Roberts, J. E. Bisi, J. C. Strum, A. J. Combest, D. B. Darr, J. E. Usary, W. C. Zamboni, K.-K. Wong, C. M. Perou, N. E. Sharpless, Multiple roles of cyclin-dependent kinase 4/6 inhibitors in cancer therapy. *J. Natl. Cancer Inst.* **104**, 476–487 (2012).
18. J. E. Bisi, J. A. Sorrentino, P. J. Roberts, F. X. Tavares, J. C. Strum, Preclinical characterization of G1T28: A novel CDK4/6 inhibitor for reduction of chemotherapy-induced myelosuppression. *Mol. Cancer Ther.* **15**, 783–793 (2016).
19. D. B. Longley, D. P. Harkin, P. G. Johnston, 5-Fluorouracil: Mechanisms of action and clinical strategies. *Nat. Rev. Cancer* **3**, 330–338 (2003).
20. C. Lerner, D. E. Harrison, 5-Fluorouracil spares hemopoietic stem cells responsible for long-term repopulation. *Exp. Hematol.* **18**, 114–118 (1990).

21. D. E. Harrison, C. P. Lerner, Most primitive hematopoietic stem cells are stimulated to cycle rapidly after treatment with 5-fluorouracil. *Blood* **78**, 1237–1240 (1991).
22. I. Beerman, C. Bock, B. S. Garrison, Z. D. Smith, H. Gu, A. Meissner, D. J. Rossi, Proliferation-dependent alterations of the DNA methylation landscape underlie hematopoietic stem cell aging. *Cell Stem Cell* **12**, 413–425 (2013).
23. G. de Haan, B. Donte, C. Engel, M. Loeffler, W. Nijhof, Prophylactic pretreatment of mice with hematopoietic growth factors induces expansion of primitive cell compartments and results in protection against 5-fluorouracil-induced toxicity. *Blood* **87**, 4581–4588 (1996).
24. T. Cheng, N. Rodrigues, H. Shen, Y.-g. Yang, D. Dombkowski, M. Sykes, D. T. Scadden, Hematopoietic stem cell quiescence maintained by $p21^{cip1/waf1}$. *Science* **287**, 1804–1808 (2000).
25. A. Ehninger, T. Boch, H. Medyouf, K. Mudder, G. Orend, A. Trumpp, Loss of SPARC protects hematopoietic stem cells from chemotherapy toxicity by accelerating their return to quiescence. *Blood* **123**, 4054–4063 (2014).
26. G. J. Peters, J. Lankelma, R. M. Kok, P. Noordhuis, C. J. van Groeningen, C. L. van der Wilt, S. Meyer, H. M. Pinedo, Prolonged retention of high concentrations of 5-fluorouracil in human and murine tumors as compared with plasma. *Cancer Chemother. Pharmacol.* **31**, 269–276 (1993).
27. K. W. Orford, D. T. Scadden, Deconstructing stem cell self-renewal: Genetic insights into cell-cycle regulation. *Nat. Rev. Genet.* **9**, 115–128 (2008).
28. S. J. Morrison, A. M. Wandycz, K. Akashi, A. Globerson, I. L. Weissman, The aging of hematopoietic stem cells. *Nat. Med.* **2**, 1011–1016 (1996).
29. G. de Haan, W. Nijhof, G. Van Zant, Mouse strain-dependent changes in frequency and proliferation of hematopoietic stem cells during aging: Correlation between lifespan and cycling activity. *Blood* **89**, 1543–1550 (1997).
30. P. J. Linton, K. Dorshkind, Age-related changes in lymphocyte development and function. *Nat. Immunol.* **5**, 133–139 (2004).
31. D. J. Rossi, D. Bryder, J. M. Zahn, H. Ahlenius, R. Sonu, A. J. Wagers, I. L. Weissman, Cell intrinsic alterations underlie hematopoietic stem cell aging. *Proc. Natl. Acad. Sci. U.S.A.* **102**, 9194–9199 (2005).
32. H. L. Chua, P. A. Plett, C. H. Sampson, B. P. Katz, G. W. Carnathan, T. J. MacVittie, K. Lenden, C. M. Orschell, Survival efficacy of the PEGylated G-CSFs Maxy-G34 and neulasta in a mouse model of lethal H-ARS, and residual bone marrow damage in treated survivors. *Health Phys.* **106**, 21–38 (2014).
33. C. Li, L. Lu, J. Zhang, S. Huang, Y. Xing, M. Zhao, D. Zhou, D. Li, A. Meng, Granulocyte colony-stimulating factor exacerbates hematopoietic stem cell injury after irradiation. *Cell Biosci.* **5**, 65 (2015).
34. L. J. Bendall, K. F. Bradstock, G-CSF: From granulopoietic stimulant to bone marrow stem cell mobilizing agent. *Cytokine Growth Factor Rev.* **25**, 355–367 (2014).
35. A. V. Ergen, M. A. Goodell, Mechanisms of hematopoietic stem cell aging. *Exp. Gerontol.* **45**, 286–290 (2010).
36. I. Beerman, W. J. Maloney, I. L. Weissmann, D. J. Rossi, Stem cells and the aging hematopoietic system. *Curr. Opin. Immunol.* **22**, 500–506 (2010).
37. H. W. Snoeck, Aging of the hematopoietic system. *Curr. Opin. Hematol.* **20**, 355–361 (2013).
38. A. Wilson, E. Laurenti, G. Oser, R. C. van der Wath, W. Blanco-Bose, M. Jaworski, S. Offner, C. F. Dunant, L. Eshkind, E. Bockamp, P. Lió, H. R. Macdonald, A. Trumpp, Hematopoietic stem cells reversibly switch from dormancy to self-renewal during homeostasis and repair. *Cell* **135**, 1118–1129 (2008).
39. A. Foudi, K. Hochedlinger, D. Van Buren, J. W. Schindler, R. Jaenisch, V. Carey, H. Hock, Analysis of histone 2B-GFP retention reveals slowly cycling hematopoietic stem cells. *Nat. Biotechnol.* **27**, 84–90 (2009).
40. C. G. Murphy, M. N. Dickler, The role of CDK4/6 inhibition in breast cancer. *Oncologist* **20**, 483–490 (2015).
41. N. Vidula, H. S. Rugo, Cyclin-dependent kinase 4/6 inhibitors for the treatment of breast cancer: A review of preclinical and clinical data. *Clin. Breast Cancer* **16**, 8–17 (2015).
42. R. G. Sheehan, E. P. Balaban, E. P. Frenkel, The impact of dose intensity of standard chemotherapy regimens in extensive stage small cell lung cancer. *Am. J. Clin. Oncol.* **16**, 250–255 (1993).
43. M. M. Rampurwala, G. B. Rocque, M. E. Burkard, Update on adjuvant chemotherapy for early breast cancer. *Breast Cancer* **8**, 125–133 (2014).
44. I. Ray-Coquard, C. Cropet, M. Van Glabbeke, C. Sebban, A. Le Cesne, I. Judson, O. Tredan, J. Verweij, P. Biron, I. Labidi, J. P. Guastalla, T. Bachelot, D. Perol, S. Chabaud, P. C. Hogendoorn, P. Cassier, A. Dufresne, J. Y. Blay; European Organization for Research and Treatment of Cancer Soft Tissue and Bone Sarcoma Group, Lymphopenia as a prognostic factor for overall survival in advanced carcinomas, sarcomas, and lymphomas. *Cancer Res.* **69**, 5383–5391 (2009).
45. J. L. Dean, C. Thangavel, A. K. McClendon, C. A. Reed, E. S. Knudsen, Therapeutic CDK4/6 inhibition in breast cancer: Key mechanisms of response and failure. *Oncogene* **29**, 4018–4032 (2010).
46. R. S. Finn, J. Dering, D. Conklin, O. Kalous, D. J. Cohen, A. J. Desai, C. Ginther, M. Atefi, I. Chen, C. Fowst, G. Los, D. J. Slamon, PD 0332991, a selective cyclin D kinase 4/6 inhibitor, preferentially inhibits proliferation of luminal estrogen receptor-positive human breast cancer cell lines in vitro. *Breast Cancer Res.* **11**, R77 (2009).
47. M. J. Niederst, L. V. Sequist, J. T. Poirier, C. H. Mermel, E. L. Lockerman, A. R. Garcia, R. Katayama, C. Costa, K. N. Ross, T. Moran, E. Howe, L. E. Fulton, H. E. Mulvey, L. A. Bernardo, F. Mohamoud, N. Miyoshi, P. A. VanderLaan, D. B. Costa, P. A. Janne, D. R. Borger, S. Ramaswamy, T. Shioda, A. J. Iafrate, G. Getz, C. M. Rudin, M. Mino-Kenudson, J. A. Engelman, RB loss in resistant EGFR mutant lung adenocarcinomas that transform to small-cell lung cancer. *Nat. Commun.* **6**, 6377 (2015).
48. The Cancer Genome Atlas Network, Comprehensive molecular portraits of human breast tumours. *Nature* **490**, 61–70 (2012).
49. B. S. Taylor, N. Schultz, H. Hieronymus, A. Gopalan, Y. Xiao, B. S. Carver, V. K. Arora, P. Kaushik, E. Cerami, B. Reva, Y. Antipin, N. Mitsiades, T. Landers, I. Dolgalev, J. E. Major, M. Wilson, N. D. Socci, A. E. Lash, A. Heguy, J. A. Eastham, H. I. Scher, V. E. Reuter, P. T. Scardino, C. Sander, C. L. Sawyers, W. L. Gerald, Integrative genomic profiling of human prostate cancer. *Cancer Cell* **18**, 11–22 (2010).
50. The Cancer Genome Atlas Research Network, Comprehensive molecular characterization of urothelial bladder carcinoma. *Nature* **507**, 315–322 (2014).
51. A. K. Witkiewicz, K. E. Knudsen, A. P. Dicker, E. S. Knudsen, The meaning of $p16^{ink4a}$ expression in tumors: Functional significance, clinical associations and future developments. *Cell Cycle* **10**, 2497–2503 (2011).
52. P. Schraml, C. Bucher, H. Bissig, A. Nocito, P. Haas, K. Wilber, S. Seelig, J. Kononen, M. J. Mihatsch, S. Dirnhofer, G. Sauter, Cyclin E overexpression and amplification in human tumours. *J. Pathol.* **200**, 375–382 (2003).
53. A. Salic, T. J. Mitchison, A chemical method for fast and sensitive detection of DNA synthesis in vivo. *Proc. Natl. Acad. Sci. U.S.A.* **105**, 2415–2420 (2008).
54. S. J. Morrison, I. L. Weissman, The long-term repopulating subset of hematopoietic stem cells is deterministic and isolatable by phenotype. *Immunity* **1**, 661–673 (1994).

Acknowledgments: We would like to thank K.-K. Wong (Dana-Farber Cancer Institute) for advice on experimental design and manuscript comments. We thank N. Fisher and the UNC Flow Cytometry Core Facility for assistance with flow cytometry analysis. Part of the animal studies was performed within the Lineberger Comprehensive Cancer Center (LCCC) Animal Studies Core Facility at the UNC at Chapel Hill. **Funding:** This work was supported by grants from NIH (AG024379, CA163896, and CA174074). The UNC Flow Cytometry Core Facility was supported, in part, by the Cancer Center Core Support Grant (P30 CA016086) to the UNC LCCC. The LCCC Animal Studies Core was supported, in part, by an NCI Center Core Support Grant (CA16086) to the UNC LCCC. **Author contributions:** S.H., P.J.R., and N.E.S conceived various aspects of the project, designed the experiments, and interpreted the results with help from J.A.S., J.E.B., and J.C.S. Preclinical experiments were performed by S.H., J.A.S., J.E.B., and P.J.R. P.J.R., K.M.M., J.A.S., H.S.-W., R.M., W.A.W., R.G.T., H.T., and E.-J.v.H. were responsible for the design, execution, and interpretation of the phase 1 healthy volunteer study. S.H., P.J.R., J.A.S., J.C.S., and N.E.S. wrote the manuscript. **Competing interests:** N.E.S. holds an equity interest in G1 Therapeutics Inc. P.J.R., J.A.S., H.S.-W., J.E.B., K.M.M., J.C.S., and R.M. were employees of the G1 Therapeutics at the time the study was conducted and have an equity interest in the company. The authors who are inventors on patents related to this work are P.J.R. and N.E.S. (Cyclin-dependent kinase inhibitors and methods of use; www.google.com/patents/US20120100100); J.C.S., J.E.B., and P.J.R. (Transient protection of normal cells during chemotherapy; www.google.com/patents/CA2906156A1?cl=en); J.C.S., J.E.B., P.J.R., and N.E.S. (Transient protection of hematopoietic stem and progenitor cells against ionizing radiation; www.google.com/patents/US20140274896); J.C.S., J.E.B., P.J.R., and N.E.S. (Hematopoietic protection against chemotherapeutic compounds using selective cyclin-dependent kinase 4/6 inhibitors; www.google.com/patents/WO2010039997A3?cl=en); and J.C.S. (CDK inhibitors; www.google.com/patents/US8598186). S.H., W.A.W., M.S., R.G.T., H.T., and E.-J.v.H. declare that they have no competing interests.

Submitted 24 January 2016
Resubmitted 14 November 2016
Accepted 27 January 2017
Published 26 April 2017
10.1126/scitranslmed.aal3986

Citation: S. He, P. J. Roberts, J. A. Sorrentino, J. E. Bisi, H. Storrie-White, R. G. Tiessen, K. M. Makhuli, W. A. Wargin, H. Tadema, E.-J. van Hoogdalem, J. C. Strum, R. Malik, N. E. Sharpless, Transient CDK4/6 inhibition protects hematopoietic stem cells from chemotherapy-induced exhaustion. *Sci. Transl. Med.* **9**, eaal3986 (2017).

Science Translational Medicine

Transient CDK4/6 inhibition protects hematopoietic stem cells from chemotherapy-induced exhaustion

Shenghui He, Patrick J. Roberts, Jessica A. Sorrentino, John E. Bisi, Hannah Storrie-White, Renger G. Tiessen, Karenann M. Makhuli, William A. Wargin, Henko Tadema, Ewoud-Jan van Hoogdalem, Jay C. Strum, Rajesh Malik and Norman E. Sharpless

Sci Transl Med **9**, eaal3986.
DOI: 10.1126/scitranslmed.aal3986

Rock-a-bye stem cells

Traditional chemotherapy can be quite effective against cancer, but its efficacy is often reduced by dose-limiting side effects. Because this type of therapy kills rapidly dividing cells, one of the most common toxicities is hematologic, resulting from chemotherapy drugs killing normal hematopoietic cells in the bone marrow. To protect the healthy hematopoietic stem cells, He *et al*. devised a method of combining chemotherapy with an inhibitor of cyclin-dependent kinases 4 and 6, which transiently suppresses the cell cycle in normal cells but not in malignant ones. The authors tested their drug with chemotherapy in mice to show protection from myelotoxicity, and they performed a human trial demonstrating its safety in healthy volunteers.